2D-Imaging of Sampling-Probe Perturbations in Laminar Premixed Flames using Kr X-ray Fluorescence

N. Hansen,[1] R.S. Tranter,[2] K. Moshammer,[1,3] J.B. Randazzo,[2] J.P.A. Lockhart,[2] P. G. Fugazzi,[1] T. Tao,[1,4] A.L. Kastengren[5]*

[1]Combustion Research Facility, Sandia National Laboratories, Livermore, CA 94551, USA

[2]Chemical Sciences and Engineering Division, Argonne National Laboratory, Argonne, IL 60439, USA

[3]Physikalisch Technische Bundesanstalt (PTB), Bundesallee 100, 38116 Braunschweig, Germany

[4]Center for Combustion Energy and Department of Thermal Engineering, Tsinghua University, Beijing 100084, PR China

[5]X-Ray Sciences Division, Argonne National Laboratory, Argonne, IL 60439, USA

submitted to:

Combust. Flame

30 Pages

8 Figures

Supplementary Material is available.

[*] Corresponding author: email: nhansen@sandia.gov; phone: +1 925 294 6272; fax: +1 925 294 2276

Abstract

The perturbation of the temperature field caused by a quartz sampling probe has been investigated in a fuel-rich low-pressure premixed ethylene/oxygen/argon/krypton flame using X-ray fluorescence. The experiments were performed at the 7-BM beamline at the Advanced Photon Source (APS) at the Argonne National Laboratory where a continuous beam of X-rays at 15 keV was used to excite krypton atoms that were added to the unburnt flame gases in a concentration of 5% (by volume). The resulting krypton X-ray fluorescence at 12.65 keV was collected and the spatially resolved signal was subsequently converted into the local temperature of the imaged spot. One and two dimensional scans of the temperature field were obtained by translating the entire flame chamber through a pre-programmed sequence of positions on high precision translation stages and measuring the X-ray fluorescence at each location. Multiple measurements were performed at various separations between the burner surface and probe tip, representing sampling positions from the preheat, reaction, and postflame zones of the low-pressure flame. Distortions of up to 1000 K of the burner-probe centerline flame temperature were found with the tip of the probe in the preheat zone and distortions of up to 500 K were observed with it in the reaction and postflame zones. Furthermore, perturbations of the temperature field have been revealed that radially reach as far as 20 mm from the burner-probe centerline and about 3 mm in front of the probe tip. These results clearly reveal the limitations of one-dimensional models for predicting flame-sampling experiments and comments are made with regard to model developments and validations based on quantitative speciation data from low-pressure flames obtained via intrusive sampling techniques.

Keywords:

low-pressure flame; speciation data, probe perturbation; X-ray fluorescence; chemical models

Introduction

Laminar premixed flames are widely used in combustion chemistry research [1]. Especially under sub-atmospheric pressure and in combination with flame-sampling molecular-beam mass spectrometry (MBMS), this flame configuration has been considered to be ideal for studying the chemical details of fuel-specific combustion processes [2, 3]. In a typical laminar premixed low-pressure flame experiment, gases are sampled through a sonic quartz nozzle from within the flame, quenched by expansion and subsequently analyzed using mass spectrometry. These data can then be converted into spatially resolved species' mole fractions as a function of distance from the burner surface when gases are sampled from multiple flame positions [1]. Pioneered by Biordi and co-workers [4, 5], flame-sampling MBMS has revealed the identity of many important combustion intermediates and provided valuable targets for the development and validation of detailed chemical models. Many chemical pathways and reaction mechanisms in flames have been identified and established by comparing the experimental results from the flame structure studies with results from model simulations [1-3, 6].

However, these flame-sampling experiments are invasive, and the sampling nozzle affects the physical and chemical structure of the flame. A description of these effects has not yet been added onto the normally used one-dimensional, laminar flame models (as implemented, for example, as PREMIX in CHEMKIN [7]), and care should be taken when comparing experimental results with model calculations [1]. In order to provide a more meaningful interpretation of the experimental and modeling results, a comprehensive physical and chemical description of the probe-induced perturbations needs to be implemented in both models and data analysis procedures.

The current understanding of the effect that a sampling probe, which is typically made out of quartz, has on a flame is that it acts as a heat sink, distorts the temperature profile and the flow field, and hence alters the species' mole fraction profiles relative to those in an unperturbed flame [1, 8, 9]. All of these effects are linked to one another; however, given the complexity of this issue, an overarching analysis of these effects has not yet been provided. Alongside theoretical considerations [10-13], experimental work has been focused on the analysis of the flow dynamics [14-16], the comparison of species profiles derived via MBMS and laser-based techniques [17-21], and the determination of composition [22] and temperature effects [8, 21, 23-26].

Accurate knowledge of the temperature is essential for interpreting the experimental observations accurately and various attempts have been made to measure the flame temperature in "perturbed" and "unperturbed" flames. These measurements, using mainly laser-based diagnostic and thermocouples, along the centerline of the flame revealed differences between the "perturbed" and "unperturbed" around 100 to 500 K in the postflame zone [8, 21, 23-26]. In the preheat and reaction zones, the temperature gradient was found to be less pronounced in the probe-distorted flame, resulting in an apparent shift of the "perturbed" temperature profile further away from the burner. While Bastin *et al.* [23] used the entire "perturbed" profile as an input to model calculations, Douté *et al.* [24], Hartlieb *et al.* [25], Vovelle *et al.* [26], and Struckmeier *et al.* [8] argued that sampling position-sensitive corrected temperature profiles best represented the temperature history an individual non-reacting atom would experience when flowing from the burner to the nozzle.

Two-dimensional probe effects on the temperature field were qualitatively visualized using NO laser-induced fluorescence by Struckmeier *et al.* [8] who concluded that temperature

gradients in the radial direction may be quite considerable and should not be ignored. Similar deviations from the one-dimensionality of the temperature field were also observed in simulations carried out by Skovorodko *et al.* [11], Gururajan *et al.* [13], and Deng *et al.* [10].

To develop a better quantitative understanding of the two-dimensional effects of the sampling probe on the temperature field, we performed synchrotron-based X-ray fluorescence (XRF) spectroscopy measurements of the gas density, from which the temperature can be calculated, around the quartz sampling probe using krypton as the fluorescent species. Highly spatially resolved raster scans of gas densities around the probe were obtained for multiple distances of the probe tip to the burner surface. The data reveal the magnitude of the two-dimensional distortions of the temperature field caused by a sampling probe compared to the unperturbed flame at an unprecedented level of detail and accuracy.

The experimental results presented in this study are intended to ultimately allow for a minimization of experimental uncertainties in flame-sampling experiments. Long term goals of these efforts are to provide guidance for probe design and empirical corrections for specific probe geometries. Ultimately, this work should result in validation targets for the detailed chemical models of the highest quality and accurate models for chemically detailed simulations. Furthermore, the results highlight the need to address two-dimensional modeling approaches for sampling results from low-pressure flame experiments.

Experimental Procedures

The experiment consists of a low-pressure flame chamber in which a vertically translatable stainless-steel McKenna-type burner (6 cm diameter) and the quartz sampling probe are mounted. The flame we used to study the probe perturbation was a fuel-rich (stoichiometry of

1.7) ethylene (C_2H_4)/O_2/Ar/Kr flame with a cold gas composition by volume of 14.5% C_2H_4, 25.5% O_2, 55% Ar, and 5% Kr at a total flow rate of 4 slm. The Kr concentration was selected to produce sufficient fluorescence signal while at the same time keeping the overall Kr usage reasonable. A shroud gas of Ar was supplied at a rate of 4 slm. The pressure in the flame chamber was kept constant at p = 30 Torr with a combination of a butterfly valve, a baratron, and a mechanical oil pump. The region behind the quartz probe was pumped by a turbo molecular pump. The design of the sampling probe is similar to those used in flame sampling studies by Hansen and co-workers [2] and is shown in the Supplementary Material (S1). All the experiments reported here used the same probe which had an opening in the tip of ~250 μm in diameter.

The experiments were performed at the 7-BM beamline of the Advanced Photon Source (APS) at the Argonne National Laboratory [27]. A schematic and a photograph of the experimental setup are shown in Fig. 1.

Details of the Kr-XRF set-up are described in Ref. [28] and only a few details are provided here. The beamline produced a nearly collimated X-ray beam of monochromatic X-rays (15 keV mean photon energy, 1.2% spectral bandpass, ~1.6×10^{11} photons/s incident flux), which was focused with a pair of 300 mm long Kirkpatrick-Baez focusing mirrors to a 5 μm × 7 μm (full width at half maximum) focus. The flame chamber was positioned so that the sampling probe was at the same z position as the beam focus. The position of the X-ray focal point at the tip of the quartz probe was defined as x = y = z = 0 mm, with the x-, y-, and z-axes defined as shown in Fig. 1(a). The beam entered and exited the flame chamber along the z-axis via thin (125 μm) polyimide windows. A diamond photodiode monitored the incident beam intensity prior to the flame chamber and a silicon PIN photodiode after the flame chamber was

used to determine the amount of absorption, particularly for locating the sampling probe in the chamber.

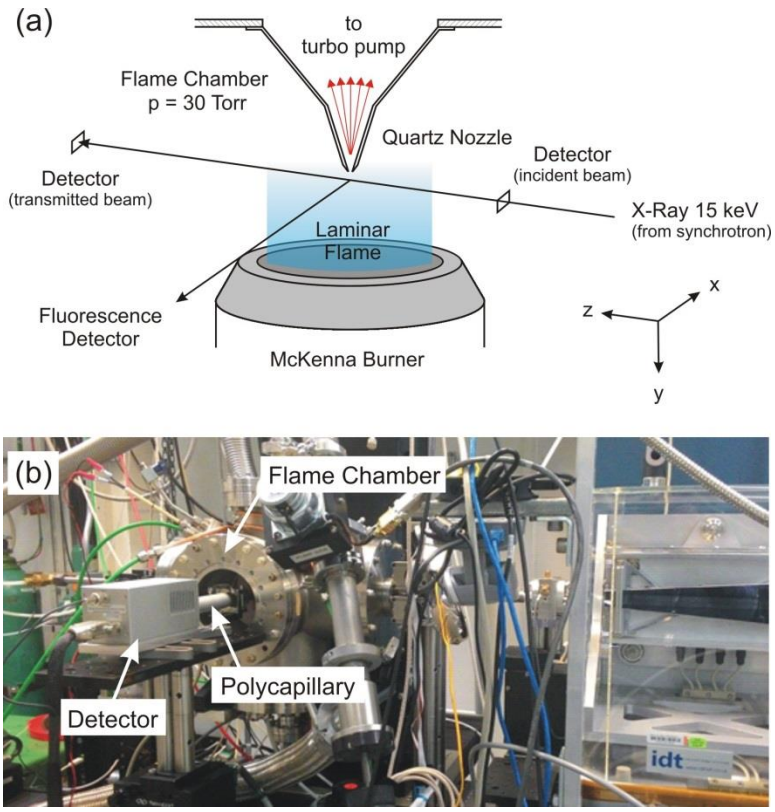

Figure 1: (a) Schematic and (b) photograph of the experimental setup. The z-axis is parallel to the X-ray beam. In the photograph the fluorescence detector and polycapillary optic are in the foreground and the X-ray beam enters from the right side.

Due to the absorption of an incident X-ray photon, the Kr in the flame is ionized, predominantly through the ejection of a K-shell (1s) electron (14.326 keV K-edge energy [29]). The resulting ion subsequently relaxes either through emission of an Auger electron or through decay of a 2p electron to the 1s level, resulting in the emission of an X-ray fluorescence photon with 12.65 keV energy (Kr Kα) [30]. These Kr fluorescence photons were collected orthogonal to the incident beam with a polycapillary X-ray optic (100 mm nominal focal length, XOS) and detected using an energy-dispersive X-ray detector (silicon drift diode, SII-Nano Vortex EM-60).

The polycapillary optic only allowed X-rays from a limited region of the beam path (300 μm FWHM) to reach the detector. As such, the measurement probes a discrete volume 5 x 7 x 300 μm FWHM in size, in a technique known as X-ray confocal microscopy [31].

One-dimensional horizontal (x) and vertical (y) scans, as well as two-dimensional raster scans, were accomplished by maneuvering the flame chamber on high-precision (better than 5 μm) translation stages around the X-ray beam while keeping the polycapillary optic and fluorescence detector fixed. The Kr-XRF signal was recorded from up to -20 to +2 mm in the x direction and -0.5 mm to HAB mm in the y direction, where HAB (height above burner) represents the multiple burner-cone separations probed. Step sizes of 200 to 250 μm were found an adequate compromise between spatial resolution and measurement time for the current experiments.

The collected fluorescence signal can be used as a measure of the gas density because the total X-ray fluorescence emission is directly proportional to the flux of the incident X-ray beam (ϕ), as measured by the diamond photodiode [see Fig. 1(a)], and the molecular density of krypton in the imaged focal point. The detected fluorescence signal S is correlated to the temperature via

$$S(x,y) \sim \phi \times x_{Kr}(x,y) \times n/V \sim \phi \times x_{Kr}(x,y) \times p/T(x,y) \quad (1)$$

where x and y are the coordinates as introduced in Fig. 1, T(x,y) is the local temperature, $x_{Kr}(x,y)$ is krypton's mole fraction at the respective flame position, and n/V is the number density that can be expressed as p/T(x,y) from the ideal gas law which is appropriate for the conditions studied. Pressure gradients do not exist in the flame and the pressure p can be considered to be constant. The fluorescence signal was typically collected for 30 s/point which resulted in point-to-point signal fluctuations that, after correction for the incident X-ray beam intensity, correlate to an accuracy of the temperature measurements of ±50 K in the postflame zone. Because of the

lower temperature and larger x_{Kr} in the preheat zone (i.e. stronger fluorescence signal), the accuracy of the temperature measurements in the preheat and reaction zone is in the order of ±20 K.

The absolute fluorescence signal was calibrated at p = 30 Torr against cold-gas (298 K) Kr-Ar mixtures of known mole fractions between x_{Kr} = 0 and 0.08; a linear response of the fluorescence signal as a function of the concentration was observed (see Supplementary Material S2). The determined calibration factor (c) was then used to calculate the flame temperatures at a constant pressure using the following equations:

$$S(x,y) = c \times \phi \times x_{Kr}(x,y) \times 1/T(x,y) \quad (2)$$

or

$$T(x,y) = c \times \phi \times x_{Kr}(x,y) \times 1/S(x,y) \quad (3)$$

$x_{Kr}(x,y)$ along the center line of the flame (x = 0 mm) was determined in separate experiments at Sandia National Laboratories using electron-ionization flame-sampling molecular-beam mass spectrometry using the instrument and routines described elsewhere [32, 33], which have been proven multiple times to retrieve accurate major species mole fraction profiles despite the temperature issues discussed in this paper. For this experiment, we used a 14.5% C_2H_4/25.5% O_2/60% Ar flame at p = 30 Torr and assumed that $1/12^{th}$ of x_{Ar} is identical to x_{Kr} in the flame studied at the APS. The x_{Kr} profile is provided in the Supplementary Material (S3). Overall, the XRF experimental signal and analysis procedure result in a combined temperature uncertainties of ±150 K in the postflame and ±50 K in the preheat and reaction zone.

For the analysis described below, it was assumed that $x_{Kr}(x,y)$ was constant along the x-axis at any given y value. However, based on the results shown in the following paragraphs, the assumption is not entirely accurate given the observed temperature distortions, which will result in concentration gradients. Thus the results presented likely underestimate the temperature

distortions somewhat and can be considered a lower limit. A complete two-dimensional simulation would be required to understand this subject entirely, but this is outside the scope of the present work.

Results and Discussion

This section is organized as follows: First, we present data from unburnt gas mixtures with known compositions to check for the applicability and validity of the experimental method. Second, we present two-dimensional images and one-dimensional vertical scans of the unperturbed flame that were taken in the absence of the sampling probe. These data serve as a reference for the measurements described in the third part, in which we discuss the two-dimensional flame perturbations at multiple burner-probe separations.

a) Cold-gas Experiments

To check for the proper performance of the experimental set-up and to calibrate the fluorescence signal, we measured the Kr X-ray fluorescence from gas mixtures with known compositions. For the results shown below, Ar and Kr at flowrates of 3850 sccm (Ar) and 200 sccm (Kr) were mixed upstream of the water-cooled McKenna-type burner through which the mixture flowed. The pressure in the flame chamber was kept constant at p = 30 Torr. For these experimental conditions Equation (1) indicates that the detectable fluorescence signal S(x,y) at any given position should be constant in the entire scanned area between the burner surface and the quartz probe tip, providing x_{Kr}, p and t remain constant. The experimental results are shown in Fig. 2(a) as a two-dimensional image around the quartz probe (with the tip positioned at 8.4 mm above the burner surface) and in Figs. 2(b) and (c) as horizontal and

vertical traces. The homogeneity observed in the two-dimensional Kr X-ray fluorescence image and the flatness of the fluorescence signal in the horizontal and vertical scans shows the suitability of the present approach to measure gas-densities in low-pressure experiments. It also demonstrates that there is no influence from the nozzle on the temperature of the cold gas mixture.

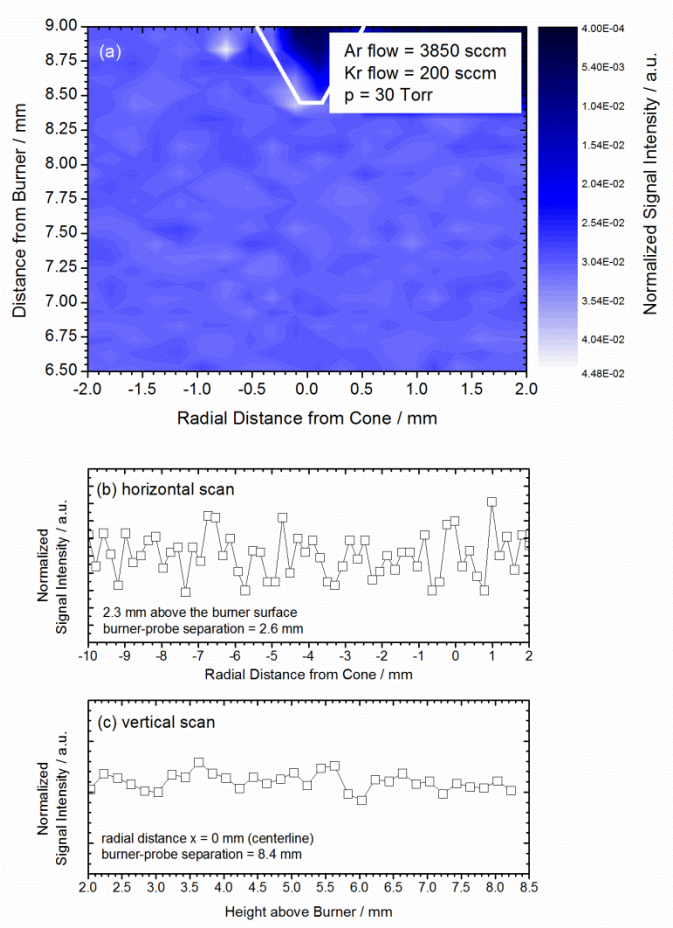

Figure 2: (a) Two-dimensional image of the Kr X-ray fluorescence from a cold gas mixture of 3850 sccm Ar and 200 sccm Kr through the McKenna-burner. The pressure was kept constant at 30 Torr and the quartz probe, as indicated in (a), was positioned 8.4 mm above the burner surface. A range from 6.5 to 9.0 mm on the y-axis and of -2.0 to 2.0 mm on the x-axis was probed. (b) Normalized Kr X-ray fluorescence signal as function of the radial distance from the cone and (c) as function of the distance from the burner surface.

b) Unperturbed Flame

Measurements of the Kr XRF were performed in the unperturbed ethylene flame by replacing the quartz sampling probe with a quartz disk. A two-dimensional raster scan was recorded from x = -12.0 to 0.0 mm and y = 23.5 to 30.0 mm above the burner surface. The result of the two-dimensional image is shown in Fig. 3(a). As can be seen a homogenous looking image was recorded, in which the signal intensity is shown with darker colors indicating smaller signal intensities. Horizontal scans from x = -12.0 to 0.0 mm at 34.0 mm and 19.0 mm above the burner surface revealed the one-dimensionality of the temperature field in the probed region. In addition, vertical one-dimensional scans were recorded at x = 0, 5.0, 12.0, 15.0, 20.0 and 25.0 mm away from the burner-probe centerline.

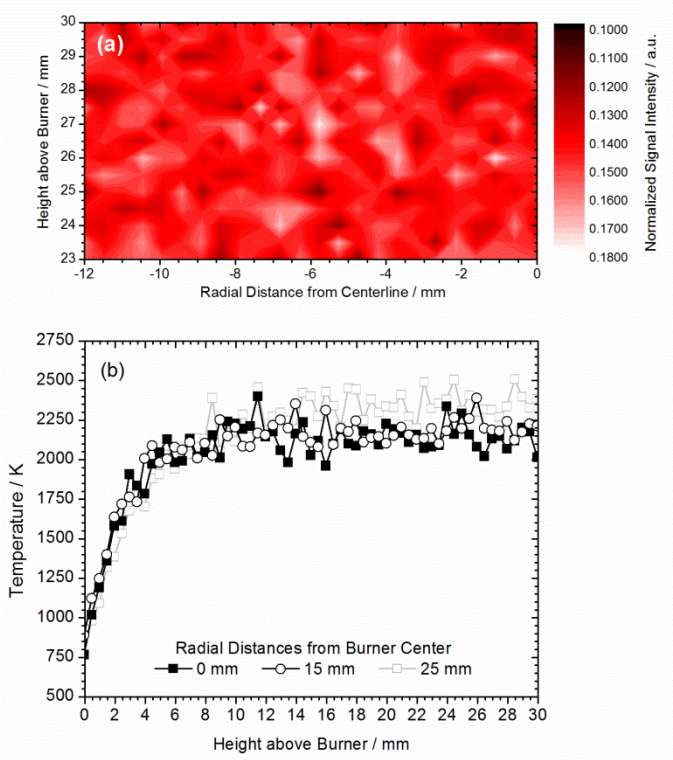

Figure 3: (a) Two-dimensional image of the Kr X-ray fluorescence from the unperturbed $C_2H_4/O_2/Ar/Kr$ flame at a pressure of 30 Torr. A range from 23.0 to 30.0 mm on the y-axis (post flame) and of -12.0 to 0.0 mm on the x-axis was probed. (b) Temperature profiles of the unperturbed flame at various radial positions: x = 0 (center line), 15.0, and 25.0 mm.

According to Eq. (3) the XRF signal can be converted into temperatures when the mole fraction x_{Kr} as a function of the x and y coordinates and the calibration factor (as determined at 298 K) are known. As described above, we used the x_{Kr}(x = 0 mm, y = 0 to 30.0 mm) from the EI-MBMS measurement (along the centerline over the burner surface) and the cold-gas (298 K) calibration data to convert the raw data into temperature profiles. The results are shown in Fig. 3(b). Fluorescence signals taken along the centerline (x = 0 mm, y = 0 to 30.0 mm) and 15.0 mm away from the centerline (x = 15.0 mm, y = 0-30.0 mm) result in nearly identical temperature profiles, indicating the flatness of the flame. The results reveal temperatures of 750 K at the burner surface and 2100 K in the exhaust region which are reasonable temperatures at these HABs for this flame. However, the vertical scans at x = 20.0 (not shown) and 25.0 mm [shown in Fig. 3(b)] reveal some deviations from the one-dimensionality of the low-pressure premixed "flat" flame. Such deviations became visible as a larger temperature in the postflame region. A likely explanation is that smaller signal intensities are observed towards the postflame zone due to shroud gas diffusing into the flame, thus resulting in a lower krypton mole fraction than at the centerline x_{Kr}.

In summary, the Kr XRF measurements in the unperturbed C_2H_4/O_2/Ar/Kr flame allowed for determining the flame's unperturbed temperature profile. In the next step, we used this unperturbed profile in combination with the Kr fluorescence measurements in the sampling-probe perturbed flame to quantify the probe-induced temperature distortion.

c) Sampling-Probe Induced Perturbed Flame

To measure the temperature drop around the quartz probe we performed scans of the Kr fluorescence from the probe-perturbed flame. An example of the experimental results is given in

Fig. 4. For this experiment, the probe burner separation was chosen to be 4.2 mm so the probe tip was in the reaction zone of the flame and the two-dimensional range from x = -12.0 to 0.0 mm and y = 4.7 to 1.5 mm was scanned. As for Fig. 3(a), the signal intensities are shown as a different color, with darker colors indicating smaller signal intensities. The sampling probe is located in the top right corner. It is immediately visible that unlike Fig 3(a) the field is no longer homogeneous in the radial direction.

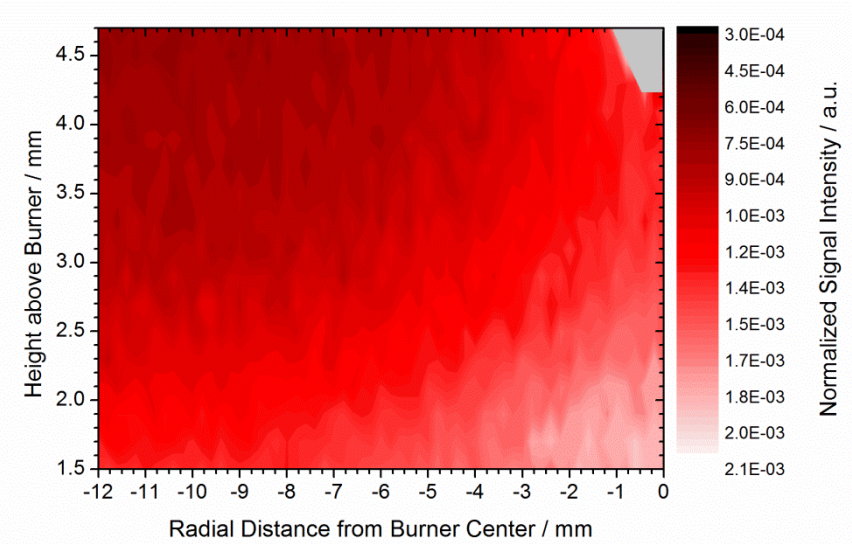

Figure 4: Two-dimensional image of the Kr fluorescence signal. The image was recorded at a burner-probe separation of 4.2 mm; a range from y = 1.5 to 4.7 mm and from x = -12.0 to 0.0 mm was scanned. Darker colors indicate smaller signal intensities.

Following the same procedures as applied for the unperturbed flame and as outlined in the "Experimental Procedures" Section, the raw XRF signals were converted into local flame temperatures. Two-dimensional images of the probe-perturbed temperature field are shown in Figs. 5(a) and (b) for burner-probe distances of 4.2 mm (reaction zone) and 2.0 mm (preheat zone), respectively. Isotherms have been added to the images to guide the readers' eyes. Large two-dimensional perturbations are immediately visible. Conversely the temperatures measured in

the unperturbed flame, Fig. 3(b), varied only in the vertical direction and isotherms ran horizontally (parallel to the burner surface) until edge effects perturbed the flow. Vertical and horizontal traces from such images of the probe-perturbed temperature fields will be discussed in the following paragraphs.

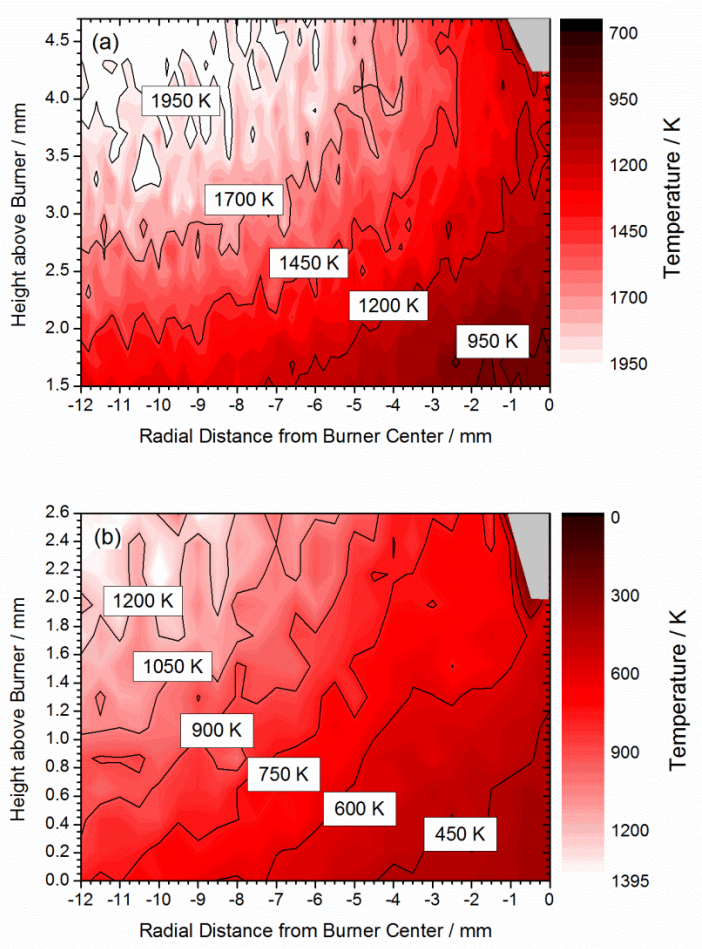

Figure 5: Two-dimensional temperature fields around the quartz probe at two different burner-probe separations: (a) 4.2 mm (reaction zone) and (b) 2.0 mm (preheat zone). Isotherms have been added to the images to guide the readers' eyes.

First, we discuss the horizontal temperature scans from x = -12.0 to +2.0 mm at a burner-probe separation of 4.2 mm. The results are shown in Fig. 6 for four different distances of the X-ray beam to the probe tip.

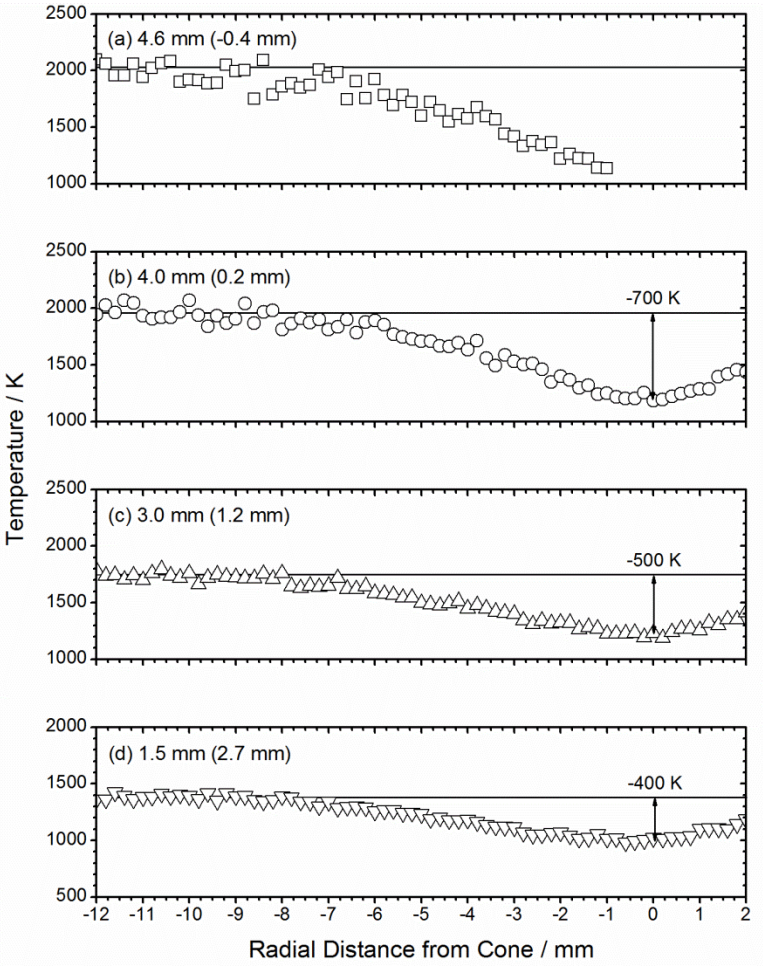

Figure 6: Temperature profiles as function of the radial and axial distance from the probe tip. The burner probe separation was kept at 4.2 mm. (a) X-ray burner separation 4.6 mm which places the probe tip below the X-ray beam and equates to a probe X-ray separation of -0.4 mm. (b) X-ray burner separation 4.0 mm = 0.2 mm in front of the tip. (c) X-ray burner separation 3.0 mm = 1.2 mm in front of the tip. (d) X-ray burner separation 1.5 mm = 2.7 mm in front of the probe tip.

Figure 6 indicates that the temperatures changes from the front of the nozzle (radial distance x = 0 mm) to the outside (unperturbed) regions by ~700 K with the X-ray beam 0.2 mm below the nozzle. The temperature change becomes smaller for larger distances away from the quartz tip, but even at a distance from 2.7 mm (1.5 mm above the burner surface), the temperature drop is still around 400 K. These results are not unexpected because similarly large numbers in the temperature drop were observed in fuel-rich propene/O_2/Ar and *n*-heptane/O_2/Ar

flames [24, 25]. More interestingly, Figs. 5 and 6 reveal significant distortions of the temperature along the radial x-axis. It can be seen that perturbations reach as far as 8 to 10 mm before the temperatures of the unperturbed flame are reached. Even larger distortions of the temperature field were observed between perturbed and unperturbed flames when "sampling" from the preheat zone [Figure 5(b)]. Here, deviations from the unperturbed flame were revealed that reach as high as 900 K when comparing the temperature in front of the nozzle to the unperturbed flame temperature shown in Fig. 3(b) at 2 mm. From the non-horizontal behavior of the isotherms shown in Fig. 5(b) over the scanned region, it is obvious that the perturbations extend beyond 12.0 mm away from the centerline (see below).

Based on these results and to show the effect of the burner-probe separation on the temperature distortions, we have performed horizontal fluorescence scans for burner-probe separations of 2.4, 4.2, and 31.0 mm, representing "sampling" from the preheat, reaction, and postflame zones. For this, scans were recorded at 0.2 mm below the tip of the probe in the range from x = -24.0 to +2.0 mm for the 2.4 mm separation and -12 to +2 mm for the 4.2 and 31.0 mm probe-burner separation. The results are shown graphically in Fig. 7. The solid lines present a Gaussian curve fit through the data. It can be seen that when sampling at 0.2 mm below the quartz probe tip, the width of the probe-perturbed range along the radial axis is different at the different burner probe separations. While at 4.2 mm the flame seems "unperturbed" around 10 mm away from the probe tip, the distortion is much wider when the probe tip is in the preheat region of the flame at 2.4 mm. In the postflame zone, the distortion appears somewhat narrower. Again, please also note the temperature drop of ~800 K in front of the probe tip when sampling in the preheat zone of the flame and the radial distortion extending ~18 mm from the centerline.

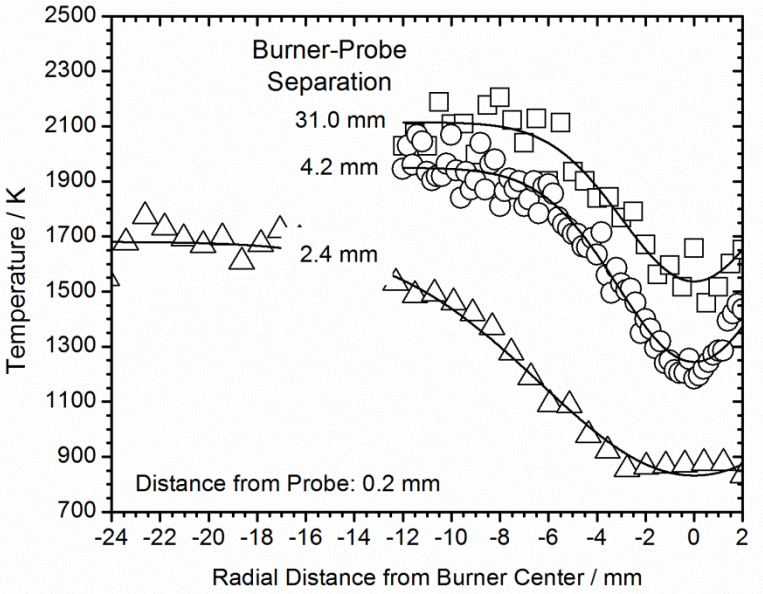

Figure 7: Distorted temperature profiles as function of the radial distance from the cone and burner-probe separations of 2.4, 4.2, and 31.0 mm. Distance of the X-ray beam to probe tip = 0.2 mm.

The observed radial distortions of the temperatures seem bothersome, considering that the overall burner radius is 30 mm and edge effects were seen as close as 20 mm from the centerline, resulting only in about 10 mm of an "unperturbed" flame. The observed horizontal temperature gradients are likely to result in concentration differences and consequently diffusion processes along the x-axis, thus supporting simulations performed by Skovorodko *et al.* [11] which revealed a significant effect of radial diffusion on the distribution of concentrations in the plane of the orifice. These results obviously indicate limitations of the currently used assumption of one-dimensionality for sampling results from low-pressure flames, as it is not obvious what temperature history the sampled molecules have experienced.

Because of the widespread use of one-dimensional flame models, vertical perturbed temperature scans (along the y-axis) on the centerline (x = 0 mm) of the perturbed flame are described next. While the interpretation of the horizontal temperature scans (along the x-axis)

was based on the assumption of a constant x_{Kr} as discussed earlier, the interpretation of the vertical scans is more complicated because x_{Kr} changes as function of the y-coordinate. Similarly to the analysis of the unperturbed flame data, the analysis of the vertical temperature scans in the perturbed flame is based on x_{Kr} along the centerline as determined by molecular-beam mass spectrometry.

The results for the probe-distorted temperature profiles on the centerline are shown in Fig. 8 for burner-probe separations of 2.0, 4.2, 7.1, 15.9, 23.5 and 31.0 mm. For the positions where the probe is in the postflame region, the temperature along the centerline as function of distance from the burner surface coincides with the unperturbed temperature profile when measurements are made at least 3-4 mm below the probe tip. In this range, the temperature steadily decreases and deviates from the unperturbed profile by up to ~500 K as seen in the previously described horizontal scans. Such long range axial perturbations were also observed theoretically by Gururajan *et al.* [13] and experimentally by Hartlieb *et al.* [25] and Struckmeier *et al.* [8]. The latter two studies revealed extreme probe perturbations to the temperature profile that extend 10-15 mm along the centerline below the probe tip. In this work the XRF technique has allowed much more detailed temperature profiles to be obtained with better spatial resolution. As a result, it can be concluded that the perturbations caused by the sampling probe, when positioned in the reaction and postflame zone of this fuel-rich flame, expand over a range of at least ±10 mm (x-axis) × 3 mm (y-axis) for the flame conditions and the current sampling probe shape.

From the results shown in Fig. 8, it is also obvious that at burner-probe distances representing "sampling" from the preheat and reaction zone the temperature profiles are significantly influenced by the sampling probe, resulting in perturbed temperatures that are

below the unperturbed temperatures even at the burner surface. These low (perturbed) temperatures are a likely explanation for the detection of typical low-temperature combustion intermediates close to the burner surface in a low-pressure n-heptane flame [34]. Furthermore, the temperature gradients in the perturbed profiles are less steep compared to the unperturbed case. These observed differences between perturbed and unperturbed temperatures at these short burner-probe distances are a likely explanation for the generally observed discrepancies between experimental and modeling results close to the burner surface.

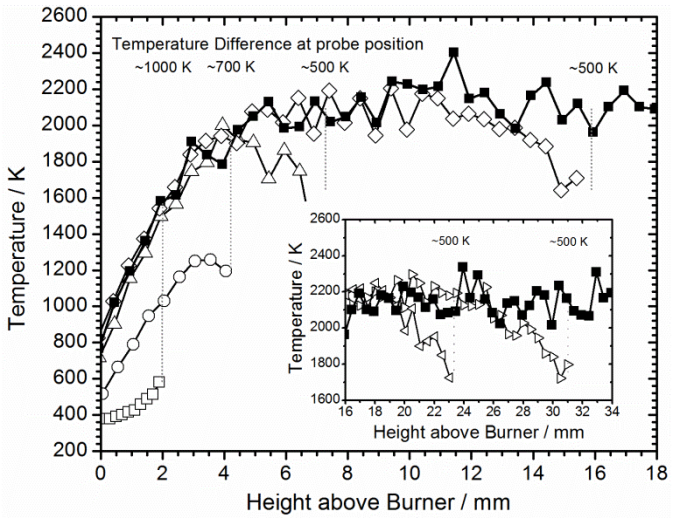

Figure 8: Perturbed (open symbols) and unperturbed (closed symbols) temperature profiles determined by X-ray fluorescence as function of the distance to the burner surface and at various sampling positions.

Furthermore, the results clearly indicate that for every sampling position, the sampled molecules experienced a different temperature history (even when radial diffusion effects are neglected). The experimental temperature profiles, measured as function of the burner-probe distance, represent the temperatures the flame gases experience when flowing from the burner to the probe tip and as such might be important input parameters for one-dimensional model

calculations. Although we have shown here that such simplified model is likely insufficient, and two-dimensional models should be developed.

Summary

We present unprecedentedly accurate, highly spatially resolved and detailed images of two-dimensional temperature fields around a quartz sampling probe in a low-pressure premixed $C_2H_4/O_2/Ar/Kr$ flame. The temperatures were determined and probe-induced perturbations revealed by Kr X-ray fluorescence from experiments that were performed at the 7-BM beamline of the Advanced Photon Source of the Argonne National Laboratory. The results clearly show how the presence of the quartz probe influences the flame temperature when sampling from the preheat, flame, and postflame region of the fuel-rich C_2H_4 flame.

Vertically, along the centerline of the burner-probe axis, temperature differences between the perturbed and the unperturbed flame in the order of 500 K were revealed in the postflame region. The drop in temperature becomes more significant in the reaction and preheat zones where differences between the perturbed and unperturbed flame of 1000 K have been detected. The flame temperatures are affected by the presence of the probe to about 4 mm in front of the sampling tip. These results are generally in good agreement with previous measurements from Hartlieb *et al.*[25], Struckmeier *et al.* [8], and theoretical considerations from Gururajan *et al.* [13].

More interestingly, the X-ray fluorescence technique allows for an accurate determination of the temperature distortions along the radial axis. A surprisingly large range of 20 mm away from the centerline appears to be affected by the presence of the sampling probe

when sampling from the preheat zone. This radial distortion becomes shorter (8-10 mm) when sampling in the reaction and postflame regions of the flame.

The presented results clearly highlight the need to develop flame models beyond the currently one-dimensional approach. Such a two-dimensional approach would eventually allow for a better description of the experimental conditions of flame-sampling experiments and consequently to more accurate insights into the ongoing combustion chemistry through providing a more realistic comparison between experimental and modeling results. In future experiments, the extent of the probe perturbations will be examined for different probe designs and flame conditions. The experiments will be designed to (a) provide more guidance towards the two-dimensional modeling approach, (b) design sampling probes that minimize the impact on the chemically detailed flame structure, and (c) develop correction rules for existing data.

Concluding Remarks

Ever since the inception of flame-sampling molecular beam mass spectrometry for flame structure analysis and the use of this chemically specific data in the form of mole fraction profiles for model validation, there has been a discussion about what temperature to use as input for model predictions. Currently the model calculations exclusively rely on the assumption of the one-dimensionality of the flame structure, thus they follow the combustion chemistry only as function of the distance to the burner surface. The presented results clearly show that the approach followed by Bastin *et al.* [23] to use the entire "perturbed" temperature profile, i.e., the temperatures measured directly in front of the nozzle, as input in the model calculations would result in an apparent shift of the temperature profile away from the burner surface and a significantly lower temperature than what the species would actually experience when flowing

through the burner to the nozzle. A more accurate input for one-dimensional model calculations would be the temperature history of the sampled gases, as it is now understood, but not implemented in current modeling approaches, that samples drawn from different flame positions relate to actually different flames.

More importantly, the experimental results presented here reveal the limitations of the simple one-dimensional approach used for model calculations and interpretations of flame-sampled data. As a consequence, caution should be used when flame-sampled mole fraction profiles serve as the only validation targets for chemical kinetic models. Given the temperature distortions and the lack of one-dimensionality of the flame, a perfect agreement between experimental and one-dimensional modeling results cannot be expected. Instead, it is recommended that two-dimensional effects should be considered when modeling the chemistry of low-pressure flame data obtained via invasive sampling techniques. Such an approach would ensure high-fidelity comparisons between experiment and model predictions.

When comparing the cost of one- vs. two dimensional flame-simulations, the computational cost needed to address two-dimensional effects might be relatively high, but the current and steadily growing computational power is expected to enable such simulations to be implemented in flame chemistry simulations to support the development of more accurate detailed chemistry mechanism. However, it is beyond the scope of the present work to show how the presented results would influence the model predictions in more sophisticated two-dimensional calculations.

Until such more sophisticated two-dimensional modeling approaches are implemented, the focus of the flame-sampling experiments should probably be more on extracting chemical insights based on the experimental data alone, e.g. species identification, rather than on the

attempt to exactly match experimental mole fraction profiles with model predictions. In this context, it is suggested that comparisons of chemical structures of flames fueled by isomeric fuels under the exact same conditions might be a valid approach to obtain insights into combustion chemistry [35-47], because the influence of the probe perturbations on the results should be identical. Furthermore, an analysis of trends in signal intensities observed in single mass spectra should allow for accessing chemical information as was recently demonstrated for flame-sampled mass spectra from opposed-flow diffusion flames [48].

Despite the described probe-perturbation issues, flame-sampling techniques should still be considered indispensable for combustion chemistry studies because they allow for an extraction of comprehensive chemical information by probing a large range of chemical structures simultaneously. It should also be pointed out that, given the combined experimental uncertainties of the invasive (probe-sampling) and non-invasive (laser-based) experimental technique, Struckmeier *et al.* [8] showed that "respectable" agreement can be achieved between invasive and non-invasive measurements of mole fractions of intermediate species.

In conclusion, for the flame-sampling data to have the highest possible impact, it seems to be advisable to reconsider the current modeling approach and to include two-dimensional effects.

Acknowledgements:

This material is based upon work supported by the U.S. Department of Energy (DOE), Office of Science, Office of Basic Energy Sciences. This research used resources of the Advanced Photon Source, a U.S. Department of Energy (DOE) Office of Science User Facility operated for the DOE Office of Science by Argonne National Laboratory. The work at Argonne was performed

under Contract No. DE-AC02-06CH11357. Sandia is a multi-mission laboratory operated by Sandia Corporation, a Lockheed Martin Company, for the National Nuclear Security Administration under contract DE-AC04-94-AL85000.

References

[1] F.N. Egolfopoulos; N. Hansen; Y. Ju; K. Kohse-Höinghaus; C.K. Law; F. Qi, *Advances and challenges in laminar flame experiments and implications for combustion chemistry.* Progr. Energy Combust. Sci. 43 (2014) 36-67.

[2] N. Hansen; T.A. Cool; P.R. Westmoreland; K. Kohse-Höinghaus, *Recent contributions of flame-sampling molecular-beam mass spectrometry to a fundamental understanding of combustion chemistry.* Prog. Energy Combust. Sci. 35 (2) (2009) 168-191.

[3] F. Qi, *Combustion chemistry probed by synchrotron VUV photoionization mass spectrometry.* Proc. Combust. Inst. 34 (2013) 33-63.

[4] J.C. Biordi, *Molecular beam mass spectrometry for studying the fundamental chemistry of flames.* Prog Energy Combust Sci 3 (1977) 151-173.

[5] J.C. Biordi; C.P. Lazzara; J.F. Papp, *Molecular beam mass spectrometry applied to determining the kinetics of reactions in flames. I. Empirical characterization of flame perturbation by molecular beam sampling probes.* Combust Flame 23 (1974) 73-82.

[6] C.S. McEnally; L.D. Pfefferle; B. Atakan; K. Kohse-Höinghaus, *Studies of aromatic hydrocarbon formation mechanisms in flames: Progress towards closing the fuel gap.* Progr. Energy Combust. Sci. 32 (3) (2006) 247-294.

[7] CHEMKIN-PRO, Reaction Design, San Diego, 2013.

[8] U. Struckmeier; P. Oßwald; T. Kasper; L. Böhling; M. Heusing; M. Köhler; A. Brockhinke; K. Kohse-Höinghaus, *Sampling probe influences on temperature and species concentrations in molecular beam mass spectroscopic investigations of flat premixed low-pressure flames.* Z. Phys. Chem. 223 (4-5) (2009) 503-537.

[9] O.I. Smith, in: Flame Structure and Processes, R. M. Fristrom, (Ed.) Oxford University Press: Oxford, 1995; pp 168-195.

[10] L. Deng; A. Kempf; O. Hasemann; O.P. Korobeinichev; I. Wlokas, *Investigation of the sampling nozzle effect on laminar flat flames.* Combust. Flame 162 (5) (2015) 1737-1747.

[11] P.A. Skovorodko; A.G. Tereshchenko; O.P. Korobeinichev; D.A. Knyazkov; A.G. Shmakov, *Experimental and numerical study of probe-induced perturbations of the flame structure.* Combustion Theory and Modelling 17 (1) (2013) 1-24.

[12] O.I. Smith, *Probe-induced distortions in the sampling of one-dimensional flames.* Combust Flame 40 (2) (1981) 187-199.

[13] V. Gururajan; F.N. Egolfopoulos; K. Kohse-Höinghaus, *Direct numerical simulations of probe effects in low-pressure flame sampling.* Proc. Combust. Inst. 35 (2015) 821-829.

[14] A.N. Hayhurst; D.B. Kittelson, *Mass-spectrometric sampling of ions from atmospheric-pressure flames. 3. Boundary-layer and other cooling of sample.* Combust. Flame 28 (2) (1977) 137-143.

[15] A.N. Hayhurst; D.B. Kittelson; N.R. Telford, *Mass-spectrometric sampling of ions from atmospheric-pressure flames. 2. Aerodynamic disturbance of a flame by sampling system.* Combust. Flame 28 (2) (1977) 123-135.

[16] A.C. Yi; E.L. Knuth, *Probe-induced concentration distortions in molecular-beam mass-spectrometer sampling.* Combust. Flame 63 (3) (1986) 369-379.

[17] D. Stepowski; D. Puechberty; M.J. Cottereau, *Use of laser-induced fluorescence of OH to study the perturbation of a flame by a probe.* Proc Combust Inst 18 (1981) 1567-1573.

[18] R.J. Cattolica; S. Yoon; E.L. Knuth, *OH concentration in an atmospheric-pressure methane-air flame from molecular-beam mass spectrometry and laser-absorption spectroscopy.* Combust Sci Technol 28 (1982) 225-239.

[19] O.I. Smith; D.W. Chandler, *An experimental study of probe distortions to the structure of one-dimensional flames.* Combust Flame 63 (1986) 19-29.

[20] D.J. Seery; M.F. Zabielski, *Comparisons between flame species measured by probe sampling and optical spectrometry techniques.* Combust Flame 78 (1989) 169-177.

[21] P. Desgroux; L. Gasnot; J.F. Pauwels; L.R. Sochet, *Correction of LIF temperature measurements for laser absorption and fluorescence trapping in a flame: Application to the thermal perturbation study induced by a sampling probe.* Appl Phys B 61 (1995) 401-407.

[22] E.L. Knuth, *Composition distortion in MBMS sampling.* Combust Flame 103 (1995) 171-180.

[23] E. Bastin; J.L. Delfau; M. Reuillon; C. Vovelle; J. Warnatz, *Experimental and computational investigation of the structure of a sooting C_2H_2-O_2-Ar flame.* Proc Combust Inst 22 (1988) 313-322.

[24] C. Douté; J.L. Delfau; R. Akrich; C. Vovelle, *Experimental study of the chemical structure of low-pressure premixed n-heptane-O_2-Ar and iso-octane-O_2-Ar flames.* Combust Sci Technol 124 (1997) 249-276.

[25] A.T. Hartlieb; B. Atakan; K. Kohse-Höinghaus, *Effects of a sampling quartz nozzle on the flame structure of a fuel-rich low-pressure propene flame.* Combust Flame 121 (2000) 610-624.

[26] C. Vovelle; J.L. Delfau; L. Pillier, *Laminar hydrocarbon flame structure.* Combust. Expl. Shock Waves 45 (4) (2009) 365-382.

[27] A. Kastengren; C.F. Powell; D. Arms; E.M. Dufresne; H. Gibson; J. Wang, *The 7BM beamline at the APS: A facility for time-resolved fluid dynamics measurements.* J Synchrotron Rad 19 (2012) 654-657.

[28] R.S. Tranter; A.L. Kastengren; J.P. Porterfield; J.B. Randazzo; J.P.A. Lockhart; J.H. Baraban; G.B. Ellison, *Measuring flow profiles in heated miniature reactors with X-ray fluorescence spectroscopy.* Proc. Combust. Inst. 36 (in press) (2016).

[29] J.A. Bearden; A.F. Burr, *Reevaluation of X-ray atomic energy levels.* Rev Mod Phys 39 (1) (1967) 125-142.

[30] J.A. Bearden, *X-ray wavelengths.* Rev Mod Phys 39 (1) (1967) 78-124.

[31] A.R. Woll; J. Mass; C. Bisulca; R. Huang; D.H. Bilderback; S. Gruner; N. Gao, *Development of confocal X-ray fluorescence (XRF) microscopy at the Cornell high energy synchrotron source.* Appl. Phys. A 83 (2) (2006) 235-238.

[32] A. Lucassen; S. Park; N. Hansen; S.M. Sarathy, *Combustion chemistry of alcohols: Experimental and modeled structure of a premixed 2-methylbutanol flame.* Proc. Combust. Inst. 35 (2015) 813-820.

[33] L. Ruwe; K. Moshammer; N. Hansen; K. Kohse-Höinghaus, *Consumption and hydrocarbon growth processes in a 2-methyl-2-butene flame.* Combust. Flame 175 (2017) 34-46.

[34] L. Seidel; K. Moshammer; X.X. Wang; T. Zeuch; K. Kohse-Höinghaus; F. Mauss, *Comprehensive kinetic modeling and experimental study of a fuel-rich, premixed n-heptane flame.* Combust. Flame 162 (5) (2015) 2045-2058.

[35] P. Osswald; U. Struckmeier; T. Kasper; K. Kohse-Höinghaus; J. Wang; T.A. Cool; N. Hansen; P.R. Westmoreland, *Isomer-specific fuel destruction pathways in rich flames of methyl acetate and ethyl formate and consequences for the combustion chemistry of esters.* J. Phys. Chem. A 111 (19) (2007) 4093-4101.

[36] N. Hansen; J.A. Miller; C.A. Taatjes; J. Wang; T.A. Cool; M.E. Law; P.R. Westmoreland, *Photoionization mass spectrometric studies and modeling of fuel-rich allene and propyne flames.* Proc. Combust. Inst. 31 (2007) 1157-1164.

[37] Y.Y. Li; L.X. Wei; Z.Y. Tian; B. Yang; J. Wang; T.C. Zhang; F. Qi, *A comprehensive experimental study of low-pressure premixed C-3-oxygenated hydrocarbon flames with tunable synchrotron photoionization.* Combust. Flame 152 (3) (2008) 336-359.

[38] J. Wang; U. Struckmeier; B. Yang; T.A. Cool; P. Osswald; K. Kohse-Höinghaus; T. Kasper; N. Hansen; P.R. Westmoreland, *Isomer-specific influences on the composition of reaction intermediates in dimethyl ether/propene and ethanol/propene flame.* J. Phys. Chem. A 112 (39) (2008) 9255-9265.

[39] N. Hansen; J.A. Miller; P.R. Westmoreland; T. Kasper; K. Kohse-Höinghaus; J. Wang; T.A. Cool, *Isomer-specific combustion chemistry in allene and propyne flames.* Combust. Flame 156 (11) (2009) 2153-2164.

[40] T. Kasper; P. Osswald; U. Struckmeier; K. Kohse-Höinghaus; C.A. Taatjes; J. Wang; T.A. Cool; M.E. Law; A. Morel; P.R. Westmoreland, *Combustion chemistry of the propanol isomers - investigated by electron ionization and VUV-photoionization molecular-beam mass spectrometry.* Combust. Flame 156 (6) (2009) 1181-1201.

[41] P. Osswald; H. Guldenberg; K. Kohse-Höinghaus; B. Yang; T. Yuan; F. Qi, *Combustion of butanol isomers - A detailed molecular beam mass spectrometry investigation of their flame chemistry.* Combust Flame 158 (1) (2011) 2-15.

[42] P. Osswald; K. Kohse-Höinghaus; U. Struckmeier; T. Zeuch; L. Seidel; L. Leon; F. Mauss, *Combustion Chemistry of the Butane Isomers in Premixed Low-Pressure Flames.* Z. Phys. Chem. 225 (9-10) (2011) 1029-1054.

[43] N. Hansen; T. Kasper; B. Yang; T.A. Cool; W. Li; P.R. Westmoreland; P. Oßwald; K. Kohse-Höinghaus, *Fuel-structure dependence of benzene formation processes in premixed flames fueled by C_6H_{12} isomers.* Proc. Combust. Inst. 33 (2011) 585-592.

[44] B. Yang; C.K. Westbrook; T.A. Cool; N. Hansen; K. Kohse-Höinghaus, *Fuel-specific influences on the composition of reaction intermediates in premixed flames of three $C_5H_{10}O_2$ ester isomers.* Phys. Chem. Chem. Phys. 13 (15) (2011) 6901-6913.

[45] B. Yang; C.K. Westbrook; T.A. Cool; N. Hansen; K. Kohse-Höinghaus, *Photoionization mass spectrometry and modeling study of premixed flames of three unsaturated $C_5H_8O_2$ esters.* Proc. Combust. Inst. 34 (2013) 443-451.

[46] M. Schenk; L. Leon; K. Moshammer; P. Osswald; T. Zeuch; L. Seidel; F. Mauss; K. Kohse-Höinghaus, *Detailed mass spectrometric and modeling study of isomeric butene flames.* Combust. Flame 160 (3) (2013) 487-503.

[47] L.-S. Tran; J. Pieper; M. Zeng; Y. Li; X. Zhang; W. Li; I. Graf; F. Qi; K. Kohse-Höinghaus, *Influence of the biofuel isomers diethyl ether and n-butanol on flame structure and pollutant formation in premixed n-butane flames.* Combust. Flame 175 (2017) 47-59.

[48] N. Hansen; M. Schenk; K. Moshammer; K. Kohse-Höinghaus, *Investigating repetitive reaction pathways for the formation of polycyclic aromatic hydrocarbons in combustion processes.* Combust. Flame in press (2017).